Electronic Supplementary Information

Highly electrical and thermoelectric properties of PEDOT:PSS thin-film via direct dilution-filtration

Jinhua Xiong,‡ Fengxing Jiang,‡ Weiqiang Zhou, Congcong Liu and Jingkun Xu*

[a] Department of Physics, Jiangxi Science and Technology Normal University, Nanchang 330013, China

E-mail: xujingkun@tsinghua.org.cn

‡ These authors contributed equally to this work.

1. Experimental

A 100 μL pristine PEDOT:PSS aqueous solution (Clevios PH1000) was added into an 3.0 mL organic solvent with ultrasonic dispersion for 30 min. Methanol (MeOH), ethanol (EtOH), isopropanol (IPA), N,N-dimethylformamide (DMF), dimethylsulfoxide (DMSO), ethylene glycol (EG) and N-methyl-2-pyrrolidone (NMP) with different boiling point are chosen as dilution and their physicochemical properties are showed in Table S1. The flexible PEDOT:PSS thin-film were prepared by a direct suction filtration with a poly(vinylidene fluoride) (PVDF) membrane (pore size: 0.2 μm) followed by drying at 60 ^{o}C for 10 h. The thin-films prepared with H_2O, MeOH, EtOH, IPA, DMF, DMSO, EG, and NMP were denoted as P100-H_2O, P100-MeOH, P100-EtOH, P100-IPA, P100-DMF, P100-DMSO, P100-EG, and P100-NMP, respectively. For comparison, the post-treated PEDOT:PSS thin-film were obtained by dipping an organic solvent on P100-H_2O and drying directly in vacuum oven at 60 ^{o}C. Additionally, the spin-coated PEDOT:PSS thin-film were prepared on a glass substrate at 1000 rpm for 30 s with a film thickness of about 208 nm. The similar dip-treatment were performed with different organic solvents.

2. Characterization

The particle size and distribution of PEDOT:PSS in organic solvents were detected with a PSA NANO2590 laser particle size instrument. The film thickness were measured by using SEM with a dual-beam focused ion beam (FIB, Helios 450S) technique. The chemical compositions and microstructure of PEDOT:PSS were analyzed by X-ray photoelectron spectroscopy (XPS, Thermo Scientific Theta Probe), atomic force microscopy (AFM, Bruker Dimension icon ScanAsyst), and UV spectroscopy (Analytikjena Specord 200). The carrier concentration and mobility were obtained by HMS-3000. The determination of electrical conductivity (σ) was performed by the standard four-probe method using a semiconductor characterization system (Keithley 2700 and 4200). The Seebeck coefficient (S) was obtained by an induced thermoelectric voltage (ΔV) in response to an applied temperature drop (ΔT= 5 K) between PEDOT:PSS films ($L \times W$= 1.2 cm × 0.5 cm) and derived as $S=\Delta V/\Delta T$.

3. Parameters

Table S1. Physical properties of diluent solvents at room temperature

Diluent solvent	Boiling pt./ °C	Dielectric constant	Absolute viscosity/cp
Water (H_2O)	100	78.5	0.89
Methanol (MeOH)	64	32.6	0.6
Ethanol (EtOH)	78	22.4	1.1
Iso Propyle Alcohol (IPA)	82	18.3	2.0
Dimethyl Formamide (DMF)	153	38.3	0.9
Dimethylsulfoxide (DMSO)	189	47.2	2.0
Ethylene glycol (EG)	197	37.7	16
N-methyl-2-pyrrolidone (NMP)	203	32.2	1.6

Table S2. Particle size distribution of 100 μL PEDOT:PSS aqueous solution in 3.0 mL different solvents.

Diluent solvent	Size distribution interval of main particles [b] /nm	Ratio of main particle number [b] /%	Average particle size [b] /nm	Thickness of PEDOT:PSS on PVDF [c] /nm
Pristine	-	-	20~30 [a]	208±6 [d]
H_2O	220~400	94.3	446	238±12.5
Methanol (MeOH)	350~1200	86.1	657	241±12.8
Ethanol (EtOH, 50 μL PEDOT:PSS)	250~1300	73.6	545	237.2±14.7
Ethanol (EtOH, 100 μL PEDOT:PSS)	300~1100	95.8	455	431.1±16.2
Ethanol (EtOH, 200 μL PEDOT:PSS)	295~850	93.7	440	987.8±25.5
Iso Propyle Alcohol (IPA)	255~825	87.3	319	235.9±15.7
Dimethyl Formamide (DMF)	250~650	99.6	354	229.3±15.1
Dimethylsulfoxide (DMSO)	200~750	76.7	257	227.6±13.7
Ethylene glycol (EG)	190~712	75.9	297	230.1±13.2
N-methyl-2-pyrrolidone (NMP)	165~300	88.9	283	235.3±16.3

[a] Provided by Heraeus Co.

[b] The data were obtained with the diluted PEDOT:PSS solution before dilution-filtration.

[c] The Thickness of PEDOT:PSS nanofilm on PVDF after dilution-filtration and drying.

[d] The pristine PEDOT:PSS thin-film were obtained on a glass substrate at 1000 rpm for 30 s.

4. Thin-film thickness

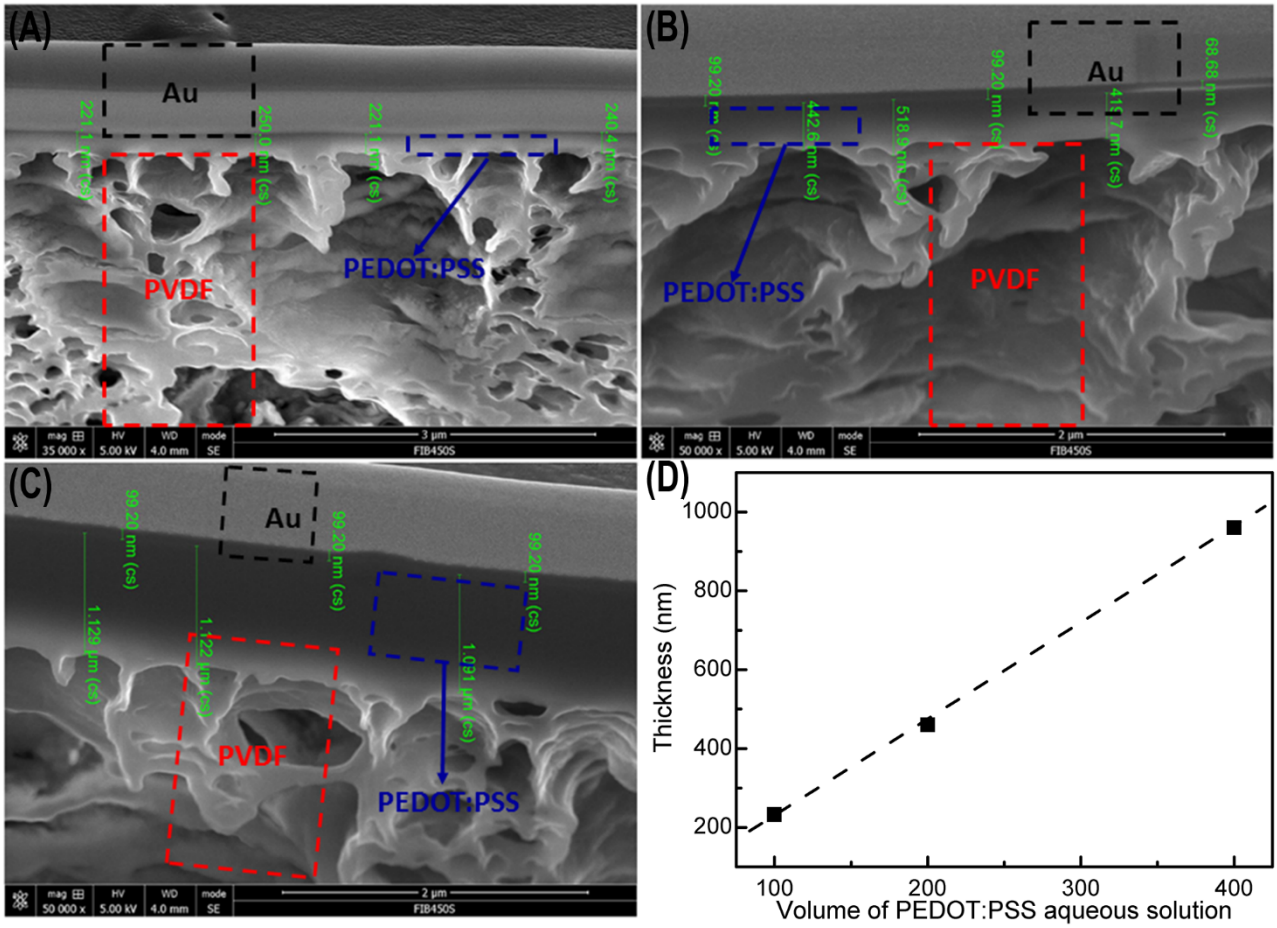

Fig. S1 The SEM images of P100 (A), P200 (B), and P400 (C) at the cross section of samples. The thickness of PEDOT:PSS thin-film on PVDF depends on the volume of original PEDOT:PSS aqueous solution with 3.0 mL ethanol as dilution (D).

The SEM images were obtained by coating Au layer on the PEDOT:PSS surface to protect it. Then, the dual-beam focused ion beam (FIB, Helios 450S) technique was used to fabricate cross section of PEDOT:PSS. The SEM was performed in FIB machine to take SEM images and measure the PEDOT:PSS thickness. The 100, 200, and 400 μL original PEDOT:PSS aqueous solution (PH1000) were diluted in 3.0 mL ethanol and filtered by PVDF (pore size: 0.2 μm), which have the average thickness of 233, 460, and 967 nm, respectively. The thickness of PEDOT:PSS shows a good linear relation with the volume of original PEDOT:PSS aqueous solution on PVDF surface.

5. XPS

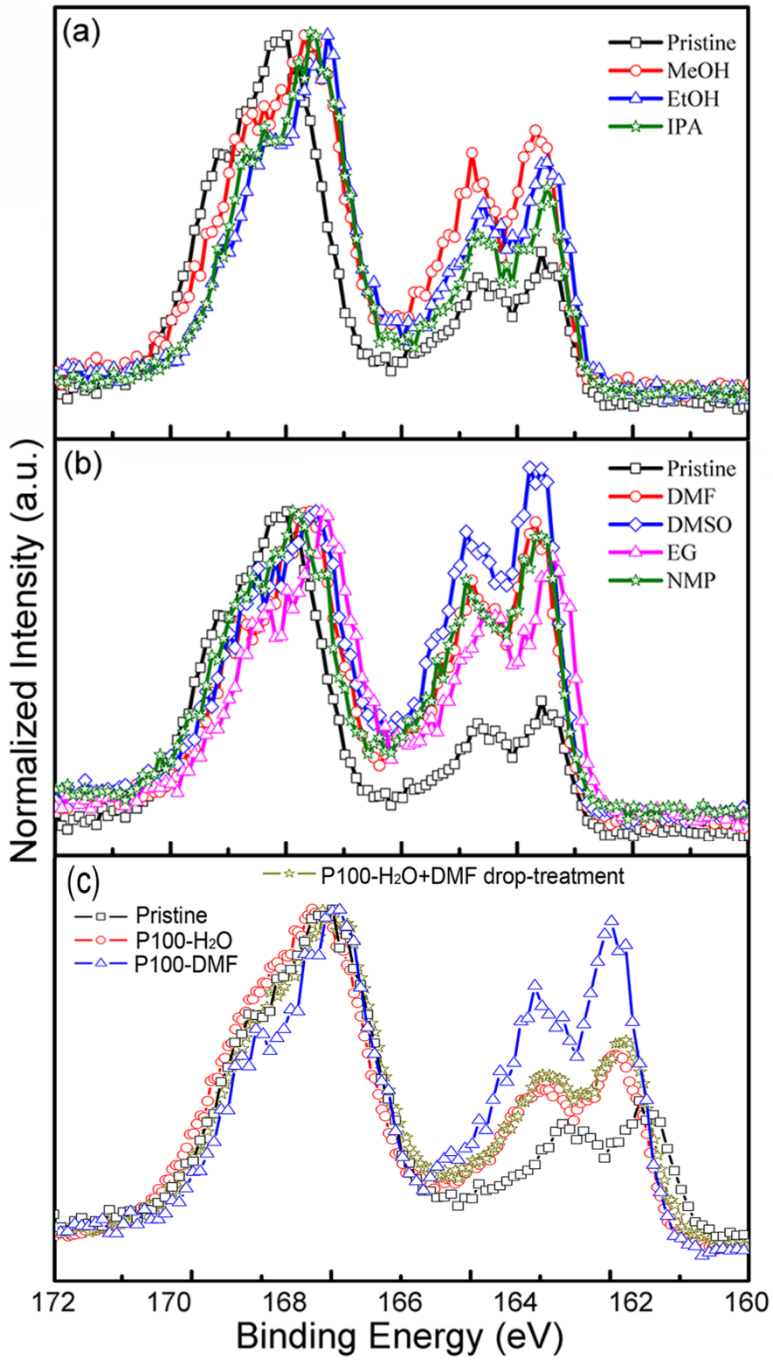

Fig. S2 S(2p) XPS spectra of PEDOT:PSS thin-films.

Fig. S2a and Fig. S2b shows the XPS of the pristine and dilution-filtration PEDOT:PSS nanofilms. Fig. S2c shows the XPS of PEDOT:PSS thin-films with different treatment methods. The pristine PEDOT:PSS film was obtained by dropping the pristine PEDOT:PSS aqueous solution on a glass substrate without any treatment. The P100-H_2O+DMF sample was prepared by dropping the DMF on the surface of P100-H_2O. The obvious differences can be observed on

the intensity of the sulfur S(2p) signals. The diluted PEDOT:PSS with DMF (P100-DMF) has a larger change compared to that of P100-H_2O with DMF drop-treatment. It indicates that the PSS content obviously decreases due to the partial dissolution of PSS in diluents.[1-3] There is no obvious difference between P100-H_2O and DMF-treated P100-H_2O. It suggests that the drop-treatment has a limited ability for the depletion of PSS from PEDOT:PSS solid thin-films.

6. Raman

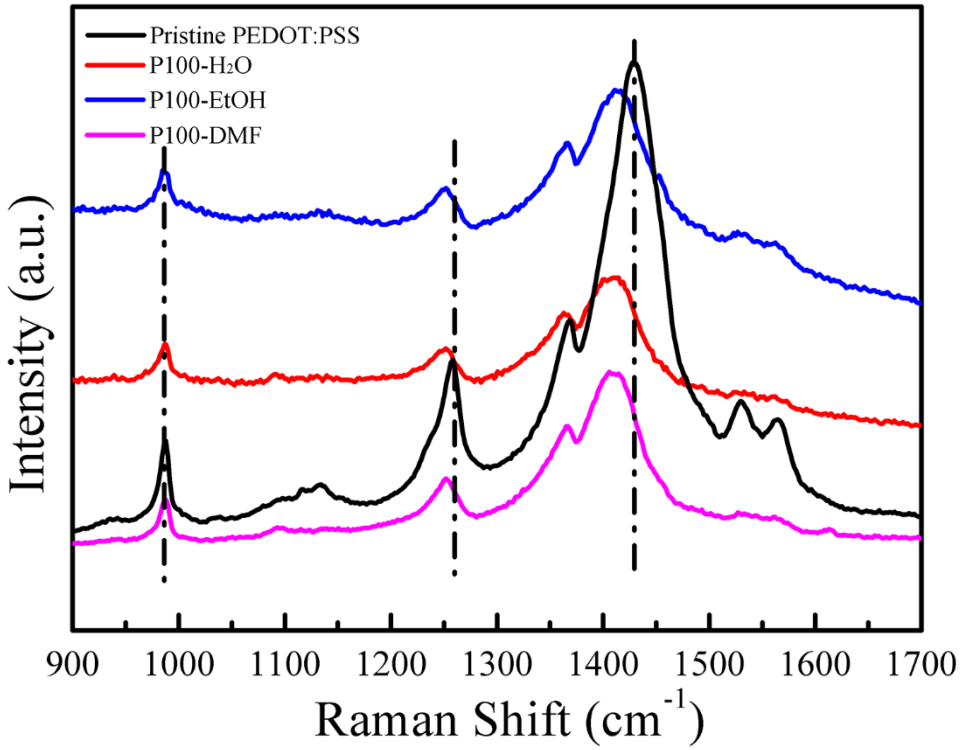

Fig. S3 Raman spectrum of different PEDOT:PSS thin-films.

The Raman spectra of pristine PEDOT:PSS displays several peaks from 400 cm^{-1} to 1800 cm^{-1}. The peaks at 1263 cm^{-1} and 1373 cm^{-1} are responsible to the ring stretching vibration (C-C). The peaks at 1436 cm^{-1} and 1534 cm^{-1} are ascribed to C=C stretching.[4,5] The diluent-treatment samples of P100-H2O, P100-EtOH, and P100-DMF show the similar profile to pristine PEDOT:PSS. Obviously, a 25 cm^{-1} red shift for P100 can be seen at 1420 cm^{-1} compared to pristine PEDOT:PSS. It indicates that the PSS content reduces in PEDOT:PSS solid thin-film including the decreasing intensity for the $C_{\alpha}=C_{\beta}$ stretching vibration (1429 cm^{-1}).[6]

7. UV-Vis-NIR

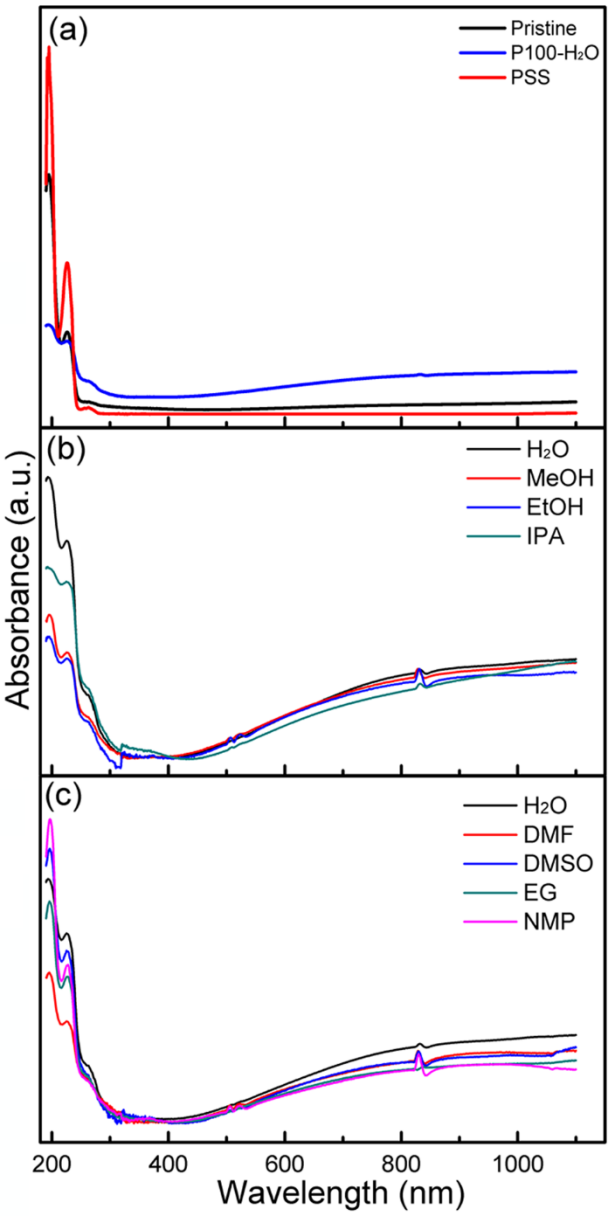

Fig. S4 UV-Vis-NIR spectra of PSS and PEDOT:PSS thin-films with different solvents as diluent. Pristine sample is obtained by spin-coating method with PEDOT:PSS aqueous solution.

Fig. S4 shows the UV-Vis-NIR absorption spectra of PEDOT:PSS thin-films with differnet organic solvent diluent-treatment. It can be seen that the two absorption bands between 190 and 250 nm originate from the aromatic rings of PSS.[7,8] The decreasing absorption bands (190~250 nm) indicate the a decreasing content of PSS in solid film. There is no obvious change from

400 to 1100 nm, suggesting that the oxidation state level of PEDOT:PSS remains unchanged and the resulting PEDOT:PSS is still a typical feature of polaron state.[9]

8. AFM

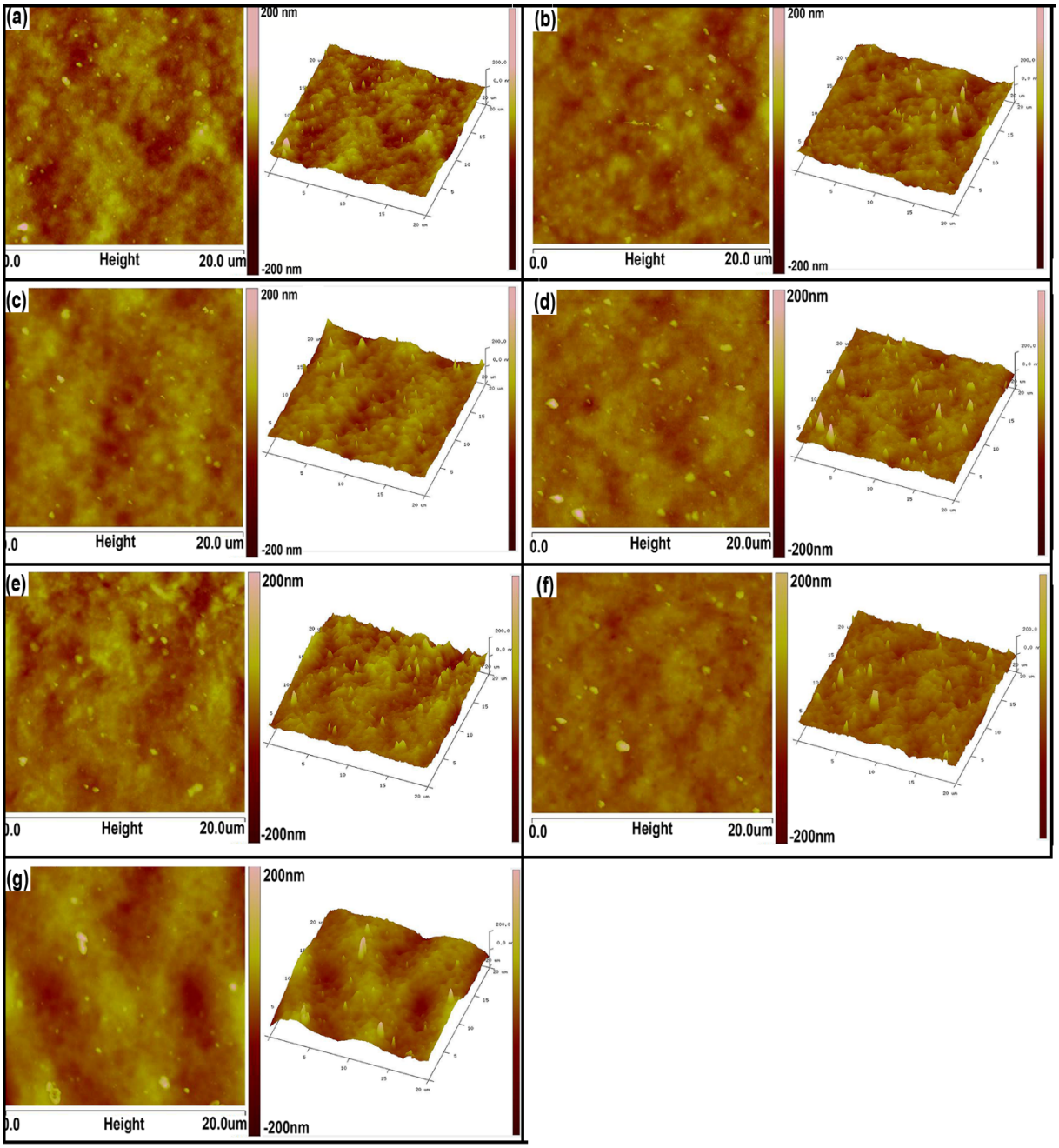

Fig. S5 Topography images of PEDOT:PSS thin-films obtained by suction filtration with MeOH (a), EtOH (b), IPA (c), DMF (d), DMSO (e), EG (f), and NMP (g) as dilution.

9. VRH

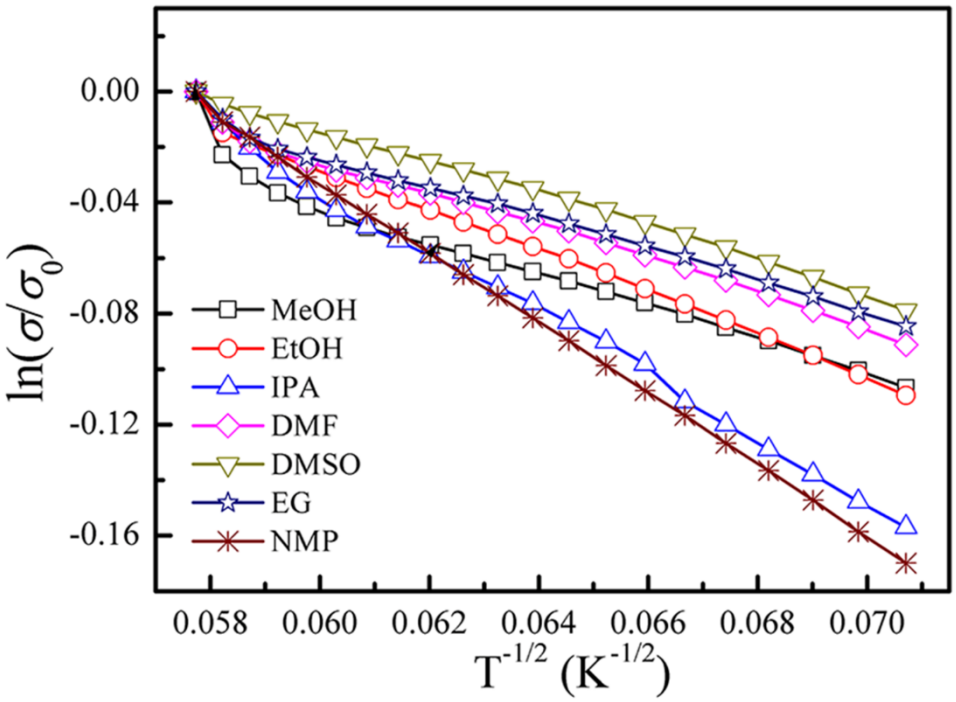

Fig. S6 The variable range hopping (VRH) analyses of *T* dependences of the σ,of P100 with different organic solvents.

10. Electrical conductivity (σ)

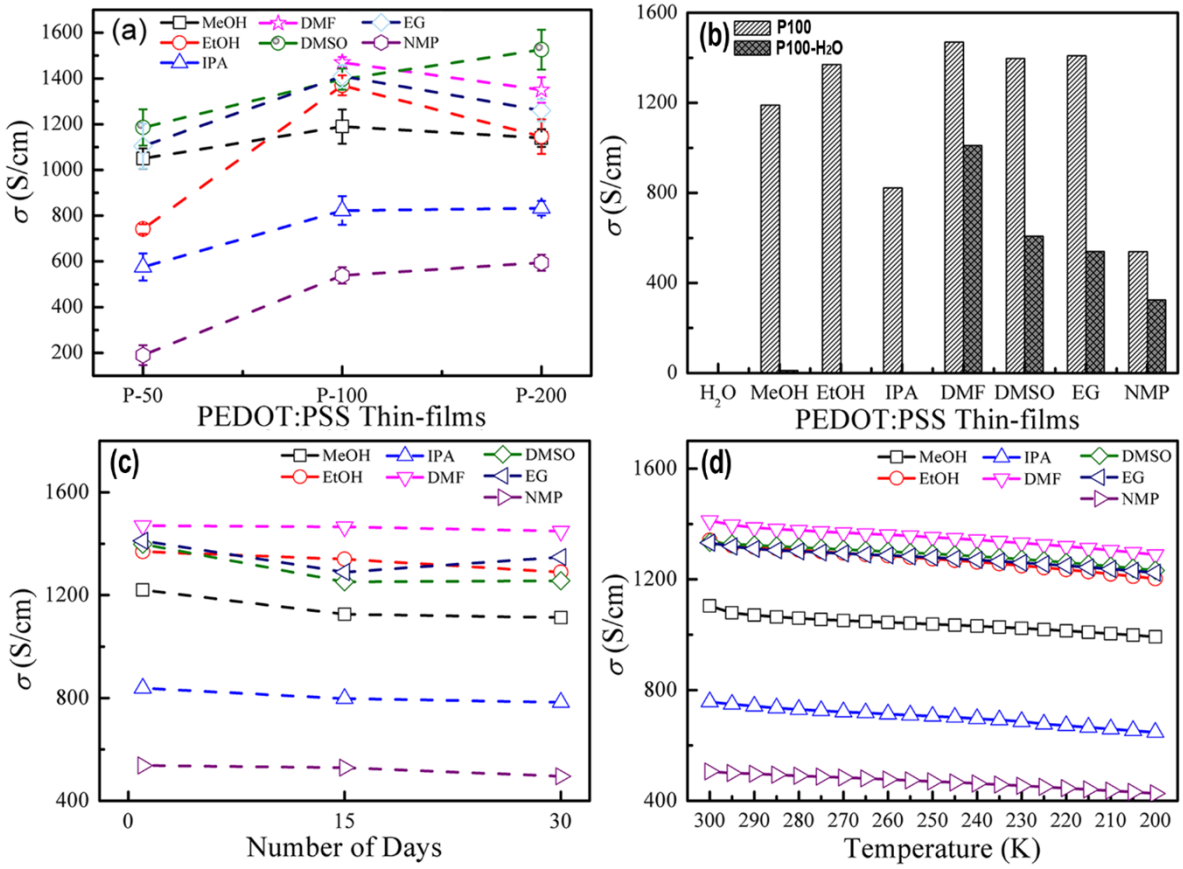

Fig. S7 The σ of P100 (a), P100 and P100-H_2O (b) samples obtained using different solvents as diluents. The time variation of σ for P100 samples (c). Temperature dependence of σ of P100 samples (d).

Fig. S7a presents the σ dependence on thin-film thickness of PEDOT:PSS. We found that the σ of thin-film maintains stable with a 100 μL pristine PEDOT:PSS aqueous solution. The lower σ is due to the inhomogeneous surface structure of thin-film without enough quantity of PEDOT:PSS. Therefore, the P100 was chosen as the main testing samples. Fig. S6b contrasts the σ of PEDOT:PSS thin-film with diluent-treatment and drop-treatment based on the P100-H_2O. It can be found that the P100 with diluent-treatment has a higher σ than the drop-treated P100-H_2O with the corresponding organic solvents. This suggests that the diluent-treatment has a more positive effect on the enhancement of σ. It is attributed to the amount of depleted PSS leading to the aggregation of PEDOT-rich nanoparticles and segregation of PSS from

PEDOT:PSS, which can be obtained based on the XPS in Table 1. On the other hand, one can see that the high boil point solvents (DMF, DMSO, EG, and NMP) show a positive influence on the σ of P100-H_2O, yet no striking enhancement are achieved for the low boil point solvents. Kim *et al.*[10] analyzed that the screening effect of the solvent (DMSO and DMF) plays an important role for the variation of the σ of PEDOT:PSS thin-film, which can reduce the Coulomb interaction between positively charged PEDOT and negatively charged PSS. Compared to the high boil point solvents, the low ones (MeOH, EtOH, and IPA) are unable to bring the screening effect due to their quick evaporation and lead to the necessary morphology change.[7] To test the stability of σ, the P100 samples were kept in ambient atmosphere for 15 and 30 days. As shown in Fig. S6c, the σ still remain 90% of the initial value, indicating a good long-term stability. Figure S6d presents the σ dependence on the temperature from 300 to 200 K. The decreasing σ as the decrease of temperature suggests that the PEDOT:PSS thin-film is a *p*-type material. Based on Fig. S6d, temperature dependences of σ can be fitted well by one dimensional (1D) variable range hopping (VRH) model.[11,12] The calculated σ of PEDOT:PSS thin-film are recorded in Table 1 and Table S3 according to $\sigma = ne\mu$, where, n is carrier concentration, μ is mobility, and e is electric charge.

Table S3. The carrier concentration and mobility of PEDOT:PSS thin-films with drop-treatment of different organic solvents.

Solvent	Carrier concentration / $\times 10^{22}$ # cm^{-3}	Mobility / $cm^2\ V^{-1}\ s^{-1}$	$\sigma^{a)}$ /S cm^{-1}	$\sigma^{b)}$ /S cm^{-1}
Methanol (MeOH)	7.41	0.02	237	11.3
Ethanol (EtOH 80%:H_2O 20%)	2.09	0.19	635	122
Iso Propyle Alcohol (IPA)	-	-	-	1.95
Dimethyl Formamide (DMF)	1.78	0.22	627	1011
Dimethylsulfoxide (DMSO)	1.40	0.40	896	608
Ethylene glycol (EG)	3.07	0.21	1031	540
N-methyl-2-pyrrolidone (NMP)	-	-	-	325

[a)] The values are calculated based on $\sigma = ne\mu$; [b)] The values are the measurement results.

11. Seebeck coefficient (*S*)

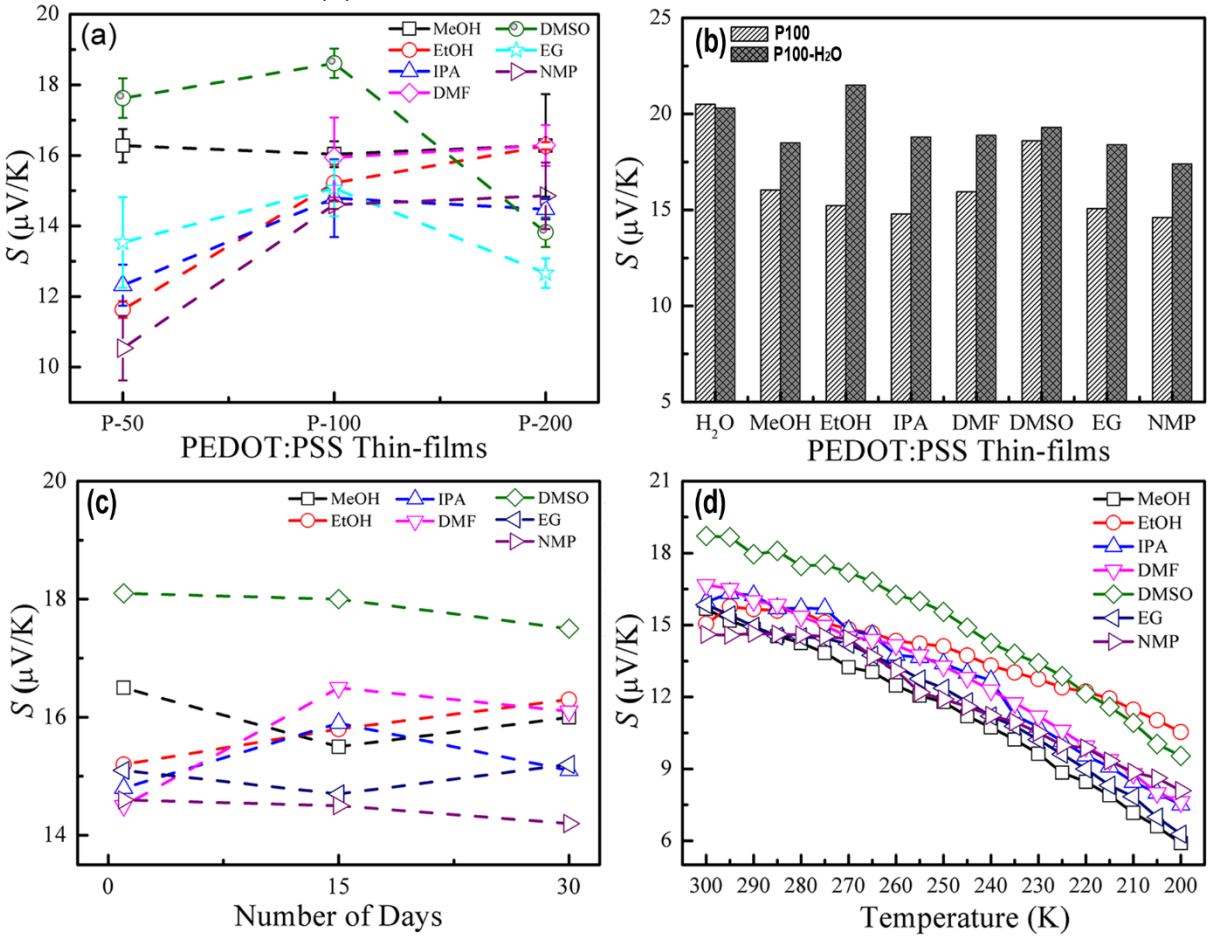

Fig. S8 The *S* of P100 (a), P100 and P100-H_2O (b) samples obtained using different solvents as diluents. The time variation of *S* for P100 samples (c). Temperature dependence of *S* of P100 samples (d).

Fig. S8a shows the *S* of PEDOT:PSS thin-film dependence on its amount. A small difference can be observed from Fig. S8b between the P100 and the drop-treated P100-H_2O samples, which is completely different from the σ. The P100 also shows the good stability of *S*. In addition, the *S* decreases as the decrease of temperature, which is in agreement with our previous results.[13,14]

12. Thermoelectric power factor ($P=\sigma S^2$) and figure of merit (ZT)

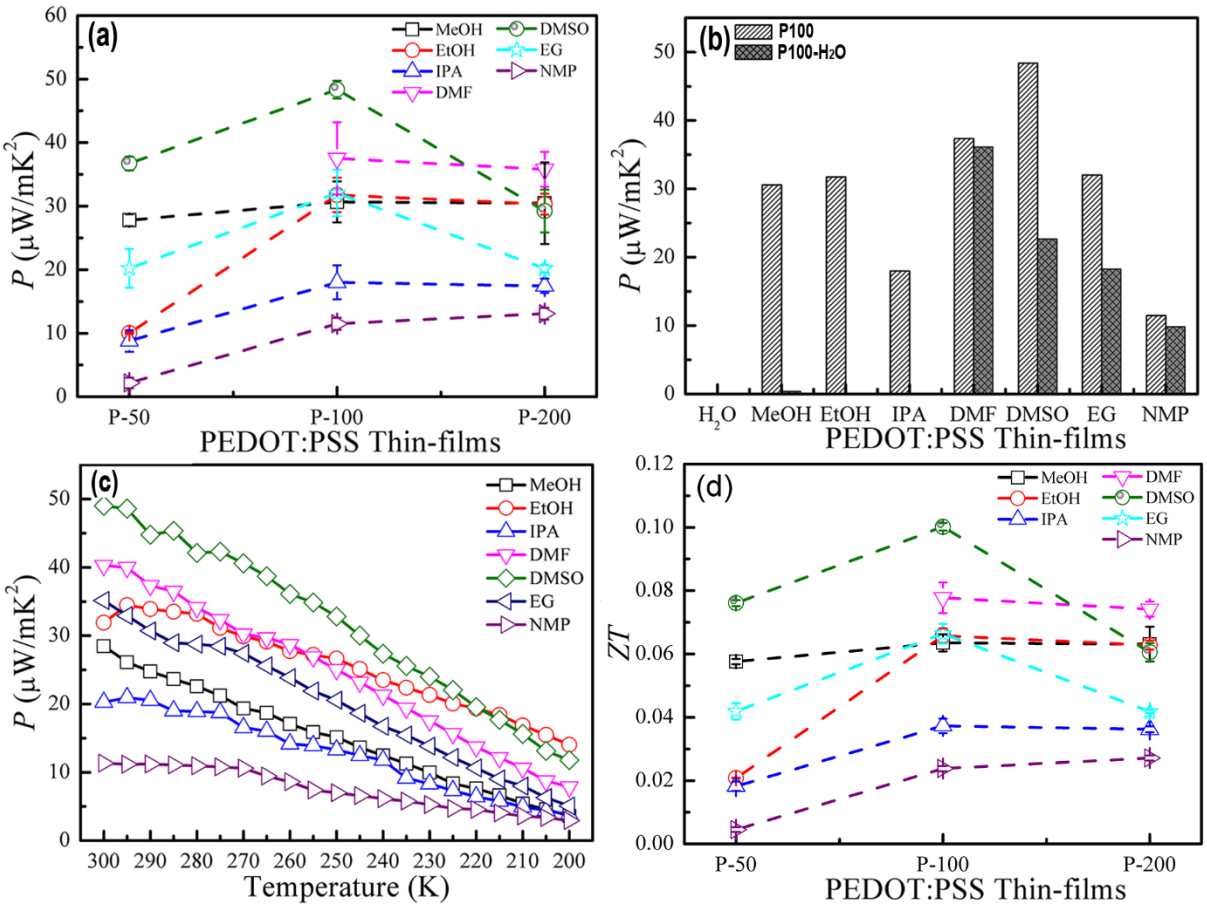

Fig. S9 The power factor of P100 (a), P100 and P100-H_2O (b) samples obtained using different solvents as diluents. Temperature dependence of electrical conductivity of P100 samples (c).

According to the values of σ and S of PEODT:PSS with different amount, the power factor was optimized in Fig. S9a. The diluent-treated P100 shows a more superior power factor compared with the drop-treated PEDOT:PSS thin-films with the corresponding organic solvents in Fig. S9b. Similar to the σ and S of PEODT:PSS, the power factor of P100 decreases as the decrease of temperature. The cross-plane (vertical) thermal conductivity ($\kappa_\perp$) in P100 was determined by a TC3010 solid thermal conductivity meter. The average $\kappa_\perp$ value of P100 with different organic solvents is 0.132 W m^{-1} K^{-1}. Based on the report by Pipe *et al.*,[1] the ratio of the in-plane thermal conductivity ($\kappa_{//}$) and $\kappa_\perp$, $\kappa_{//}/\kappa_\perp$ is about 1.40±0.22. The average $\kappa_{//}$ of P100 is 0.18 W m^{-1} K^{-1}, which is close to the results reported by Toshima *et al.*[15] (0.2 W m-

^{1} K^{-1}) and our previous report (0.17 W m^{-1} K^{-1})[16]. The maximum *ZT* is about 0.1 for P100-DMSO.

Reference

1 G. H. Kim, L. Shao, K. Zhang and K. P. Pipe, *Nat. Mater.*, 2013, **12**, 719-723.

2 X. Crispin, F. L. E. Jakobsson, A. Crispin, P. C. M. Grim, P. Andersson, A. Volodin, C. v. Haesendonck, M. V. d. Auweraer, W. R. Salaneck and M. Berggren, *Chem. Mater.*, 2006, **18**, 4354-4360.

3 Y. H. Kim, C. Sachse, M. L. Machala, C. May, L. Müller-Meskamp and K. Leo, *Adv. Funct. Mater.*, 2011, **21**, 1076-1081.

4 S. Garreau, G. Louarn, J. P. Buisson, G. Froyer and S. Lefrant, *Macromolecules*, 1999, **32**, 6807-6812.

5 O. A. Lisowska, A. P. Nowak, M. Wilamowska, M. Sikora, W. Szczerba and C. Kapusta, *Synth. Met.*, 2010, **160**, 1234-1240.

6 J. Wang, K. Cai and S. Shen, *Org. Electron.*, 2014, **15**, 3087-3095.

7 D. Alemu, H.-Y. Wei, K.-C. Ho and C.-W. Chu, *Energy Environ. Sci.*, 2012, **5**, 9662-9671.

8 Y. Xia, K. Sun and J. Ouyang, *Energy Environ. Sci.*, 2012, **5**, 5325-5332.

9 H. Park, S. H. Lee, F. S. Kim, H. H. Choi, I. W. Cheong and J. H. Kim, *J. Mater. Chem. A*, 2014, **2**, 6532-6539.

10 J. Y. Kim, J. H. Jung, D.E. Lee and J. Joo, *Synth. Met.*, 2002, **126**, 311-316.

11 Y. Xia and J. Ouyang, *ACS Appl. Mater. Interfaces*, 2012, **4**, 4131-4140.

12 J. Joo, S. M. Long, J. P. Pouget, E. J. Oh, A. G. MacDiarmid and A. J. Epstein, *Phys. Rev. B*, 1998, **57**, 9567-9580.

13 H. Shi, C. Liu, J. Xu, H. Song, B. Lu, F. Jiang, W. Zhou, G. Zhang and Q. Jiang, *ACS Appl. Mater. Interfaces*, 2013, **5**, 12811-12819.

14 C. Liu, F. Jiang, M. Huang, R. Yue, B. Lu, J. Xu and G. Liu, *J. Electron. Mater.*, 2011, **40**, 648-651.

15 N. Toshima and N. Jiravanichanun, *J. Electron. Mater.*, 2013, **42**, 1882-1887.

16 F. X. Jiang, J. K. Xu, B. Y. Lu, Y. Xie, R. J. Huang and L. F. Li, *Chin. Phys. Lett.*, 2008, **25**, 2202-2205.